Quantifying oxygen diffusion during thermal degradation of combustible porous media

Fei Hou [a, b, c], Xiaoxing Zhong [a, *], Marco A.B. Zanoni [d], Tarek L. Rashwan [b, c], José L. Torero [b, *]

[a] School of Safety Engineering, China University of Mining and Technology, Xuzhou 221116, China

[b] Department of Civil, Environmental and Geomatic Engineering, University College London, London, WC1E 6BT, UK

[c] School of Engineering & Innovation, The Open University, Milton Keynes, MK7 6AA, UK

[d] Department of Civil and Environmental Engineering, The University of Western Ontario, London, Ontario, N6A 5B9, Canada

Abstract: Oxygen diffusion controlled combustion occurs when local oxygen transport is slower than the chemistry, commonly found in porous combustible material or combustible material embedded within an inert porous medium. This mode of combustion, such as smouldering, can pose dangerous fire risks and also be harnessed in environmentally beneficial applications. However, the oxygen diffusion limitation is poorly understood in all contexts and persists as a key knowledge gap. Quantitative analysis of oxygen diffusion effects is therefore crucial for understanding the combustion behavior of combustible porous media and developing precise smouldering simulation models. In this paper, a reactive transport model incorporating both oxygen diffusion and chemical consumption was developed. Using coal as the model fuel, the impacts of key parameters on global mass loss during the one-dimensional diffusion combustion of coal samples were simulated and compared with TGA experiments conducted within a range of oxygen concentrations between 3-21%. Using this method, key kinetic and oxygen diffusion parameters were obtained within reasonable ranges by using a genetic algorithm optimization method. With these optimized parameters, the local oxygen distribution profiles in the samples at different inlet oxygen concentrations were simulated. The results indicate that oxygen diffusion

can lead to large oxygen concentration differences within the coal samples, exceeding 63% of the inlet oxygen concentration. These oxygen differences can impact the local chemistry throughout the sample, and lead to fundamental errors in analyzing global kinetic analyses, if the transport effects are not considered. Altogether, this study delivers new insights into a potentially rate-limiting phenomenon that is relevant in progressing knowledge on many fire problems and engineering applications.

Keywords: Oxygen diffusion effects; Kinetics; Intrinsic mechanism; Genetic Algorithm; TGA

Nomenclature

Y	mass fraction
m, n	reaction order
C_{O_2}	oxygen concentration, %
A	pre-exponential factor, 1/s
E	apparent activation energy, kJ/mol
R	ideal gas constant, r = 8.314 J/mol-k
T	temperature, k
$\dot{m}'$	mass loss rate, kg/kg-s
m	mass of solid material, kg/kg
t	time, s
N	amount of TGA data
D	oxygen diffusivity, m^2/s
Δt	time step, s
h	thickness of coal sample in TGA experiments
w	thickness discretization amounts
ρ_g	gas density, kg/m^3
r	radius of crucible, r = 2.75mm
$\dot{C}'_{O_2}$	oxygen chemical consumption rate, 1/kg-s
p	temporal discretization amounts
k	oxygen diffusion exponent

Greeks

v	stoichiometric coefficients of reaction, kg/kg
$\dot{\omega}'$	reaction rate, 1/kg-s
φ	calculation error, %
ε	porosity

Subscripts

O_2	oxygen
ash	ash
eg	exhaust gas
exp	experimental results
cal	calculated results

1. Introduction

Combustion within porous solid materials is complicated because of the potential coupling of heat and mass transport with degradation chemistry [1-3]. These systems may be comprised of combustible solids that are (i) themselves porous or (ii) embedded within an inert porous matrix. Recently, combustion processes occurring within a porous matrix or with porous materials, such as smouldering, have become a viable means for various environmentally beneficial applications – including waste-to-energy [4-6], bio-char production [7, 8], and contaminated soil remediation [9-12]. While oxygen can influence these combustion processes through chemistry, diffusion, and convection within the pores, local diffusion transport typically limits the rate of smouldering, resulting in the characteristic combustion time scales are consistent with diffusive processes [1]. Therefore, understanding the role of oxygen diffusion in thermal degradation of combustible porous media is paramount.

Extensive studies have explored the global impact of particle size (which affects porosity and consequently oxygen diffusion transport) on the degradation process from the perspectives of developing degradation kinetic mechanisms [13], characterizing gas products [14], and assessing the influence of micro pores [15]. However, there is limited research on the effects of local oxygen diffusion during thermal degradation of combustible porous media.

The thermal degradation induced mass loss of most complex organic solids often exhibits continuous and smooth progression in time that – in the absence of mass transport effects – can be described by modelling competing endothermic and exothermic reactions [1]. Different methodologies have been developed to isolate the key reaction steps but, given the integral nature of mass loss, it is very challenging to accurately delineate these reactions [16-19]. If oxygen diffusion also needs to be

considered, then it is even more complicated to elucidate the competing nature of oxygen diffusion and degradation chemistry.

Dakka et al. [20] observed significant variations in the components of thermogravimetric analysis (TGA) exhaust gases and provided a comprehensive explanation of mass transport effects on poly methyl methacrylate (PMMA) degradation. However, due to the fuel particle size, their study could only investigate the roles played by oxygen diffusion transport and inert degradation gas transport within different temperature ranges and with a single particle size. Song et al. [21] investigated the influences of external diffusion, inter-particle diffusion, and pore diffusion on kinetic parameters derived from TGA experiments. A strong reduction in the apparent reaction rate, up to 25.5%, was observed due to inter-particle oxygen diffusion effects. Given the assumption that the intrinsic kinetic parameters remain constant with oxygen concentrations, these results were attributed to oxygen diffusion effects. These diffusion effects resulted in lower local oxygen concentrations than those specified experimentally for the flow. Furthermore, when adjusting the inlet oxygen concentration in TGA experiments, the kinetic parameters obtained using the same method exhibited significant variations [22-24], providing additional evidence of oxygen diffusion effects.

Despite the insight provided by the above studies on oxygen diffusion effects, there are no systematic or quantitative analyses that investigate the thermal degradation dynamics of combustible porous materials under oxygen-diffusion-controlled conditions. This knowledge gap hinders the accurate development of predictive tools to understand fundamental combustion behavior relevant to both smouldering fire problems and applications.

This study aims to quantitatively analyze the influence of oxygen diffusion effects on the thermal degradation of combustible porous media, mainly focusing on coal. A novel dynamic modeling method was developed, which simulated both oxygen diffusion and chemical consumption during coal combustion. Using this model, the oxygen distribution profiles during one-dimensional combustion of coal samples at

different environmental oxygen concentrations were obtained. The results provide valuable insights into the role that oxygen diffusion can play thermal degradation, which is relevant for a wide range of thermal degradation processes.

2. Methodology

2.1 Experimental samples and procedures

Coal was selected as the model fuel for this study due to its morphology and the comprehensive nature of the existing data. Bituminous coal was used from the NO.205 working face of the Xiegou coal mine in Shanxi, China. The proximate analysis of the coal sample showed 2.98%, 13.34%, 29.4%, and 54.28% mass fractions for moisture, ash, volatile matter, and fixed carbon, respectively. In addition, the ultimate analysis showed 83.27%, 4.72%, 10.51%, 0.19%, and 1.31% mass fractions for C, H, O, S, and N, respectively. Raw coal was collected from the site and sealed for low-temperature storage prior to experimentation. When tested, the coal was stripped of its outermost layer and ground into fine particulates in a vacuum glovebox. Following best practices [21], particle sizes 0.048 to 0.075 mm were used to minimize the interference of inert degradation products transport (inside sample particles) on coal combustion.

The reference experimental configuration is the TGA; therefore, this experimental approach was followed here. An SDT-Q600 synchronous thermal analyzer (TA, American) was used to continuously monitor mass loss and heat flow during coal combustion. Fig.1 shows the configuration inside TGA analyzer and the experimental systems, which consist of a gas supply system, thermogravimetric system, and data processing system. By adjusting the mass flow ratio of oxygen and nitrogen, the inlet oxygen concentration was varied between 21%, 16%, 12%, 8%, 5%, and 3%. A 10±0.01 mg coal sample (~ 0.7 mm thick in a Φ5.5×4 mm alumina crucible) was weighed for each test. The gas flow rate was 100 ml/min. The initial temperature was 30°C, and the temperature was increased to 800°C at 5°C/min. Each test was repeated three times, and the empty crucible data was subtracted from the mass loss results.

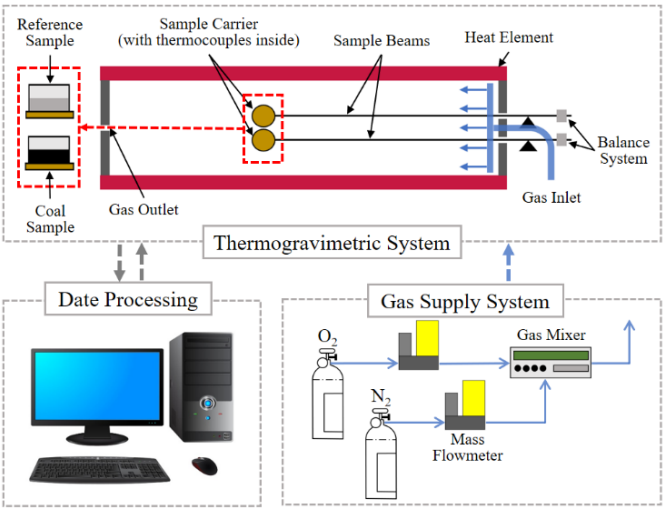

Fig.1 Schematic of the TGA experimental system

2.2 Calculation methods

Coal degradation chemistry at low temperatures is governed by slow chemical adsorption of oxygen, and therefore not strongly influenced by oxygen diffusion. Therefore, this study focused mainly on the oxygen diffusion effects at high temperatures.

A one-step equation (Eq. 1) was used to describe coal combustion at high temperatures:

$$Coal + v_{O_2} Oxygen \rightarrow v_{ash}\, Ash + v_{eg}\, Exhaust\ gas \qquad (1)$$

Assuming constant gas pressure in TGA experiments, the reaction rate of Eq.1 is only a function of temperature. This is expressed using an n-order mechanism for reactant concentrations and the Arrhenius equation:

$$\dot{\omega}' = Y_{coal}{}^{m} C_{O_2}{}^{n} A e^{-E/RT} \qquad (2)$$

It is well-established that coal undergoes many competing endothermic and exothermic degradation reactions [16, 17, 25, 26]. However, a simplified global one-step reaction was chosen to explore the potential for oxygen diffusive effects during combustion at high temperatures. Because transport phenomena are often neglected in TGA analyses, this study warranted simplified chemistry.

Following Eq. 1, Eq. 3 was derived to calculate the mass loss rate (DTG) from the TGA results. Eq.4 was used to calculate the remaining solid mass (TG) following the explicit time integration method.

$$\dot{m}'_{cal} = \dot{m}'_{coal} + \dot{m}'_{ash} = (1 - v_{ash})\dot{\omega}' m_{coal} \qquad (3)$$

$$(m_{cal})_{t_i} = (m_{coal} + m_{ash})_{t_{i-1}} + \left(\dot{m}'_{cal}\right)_{t_{i-1}} \Delta t \qquad (4)$$

Based on Eq. 3 and Eq. 4, iterative calculations were performed on the time series to obtain DTG and TG curves with respect to temperature, i.e., the 'calculated' results. These calculated results were then compared against measured results using a Genetic Algorithm (GA) to determine optimal values of the unknown kinetic parameters in Eqs.1-4 to minimize the calculation error (Eq. 5) between the calculated and experimental results.

$$\varphi = 0.5 \cdot \frac{1}{N} \sum_1^N \left[\left| \frac{m_{exp} - m_{cal}}{m_{exp}} \right|_{t_i} + \left| \frac{\dot{m}'_{exp} - \dot{m}'_{cal}}{\dot{m}'_{exp}} \right|_{t_i} \right] \times 100 \qquad (5)$$

While routine kinetic analyses using GA methods assume uniform spatial reactant concentrations (e.g., like in Section 3.1), the diffusion analyses in this study necessitated spatial discretization. In the TGA experiments, the horizontal coal sample length (5.5mm) was much larger than the vertical length (0.7mm) – see Fig.2. Therefore, the governing reactive transport equation was expressed in one dimension. Eq. 6 presents the governing equation with one-dimensional oxygen diffusive transport and chemical degradation:

$$\frac{\partial C_{O_2}}{\partial t} = D(T) \frac{\partial^2 C_{O_2}}{\partial x^2} + \dot{C}'_{O_2} \qquad (6)$$

where the temperature-sensitive oxygen diffusion coefficient is given by $D(T)=10^k T^{3/2}$, and the oxygen consumption rate is given by $\dot{C}'_{O_2}=v_{O_2} \cdot \dot{m}'_{coal}$ following Eq.1.

Along the downward combustion direction in Fig.2, the thickness of the coal sample was evenly discretized into segments, 1 to *w*. The diffusion rate of oxygen in different segments was calculated by Eq.7:

$$D(T)\frac{\partial^2 C_{O_2,j}}{\partial x^2} = \begin{cases} D(T)\dfrac{C_0 - 2C_{O_2,j} + C_{O_2,j+1}}{\Delta x^2}, & j = 1 \\ D(T)\dfrac{C_{O_2,j-1} - 2C_{O_2,j} + C_{O_2,j+1}}{\Delta x^2}, & 1 < j < w \\ D(T)\dfrac{C_{O_2,j-1} - C_{O_2,j}}{\Delta x^2}, & j = w \end{cases} \quad (7)$$

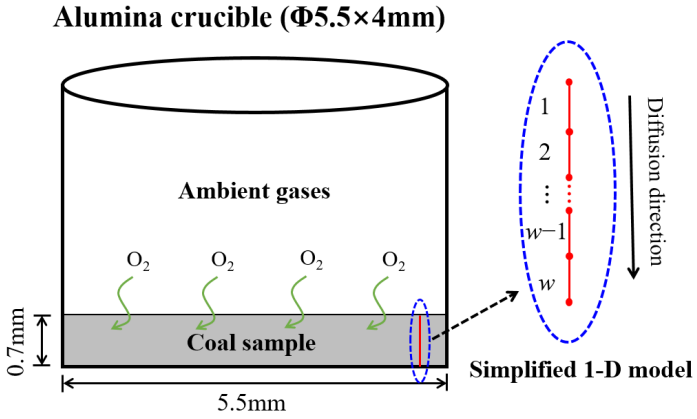

Fig.2 Schematic of coal sample diffusion and combustion in TGA experiment and the model discretization.

With the influence of oxygen diffusion, the segments near the top of the crucible experienced higher oxygen concentrations and faster reactions. Conversely, downward within the coal sample, lower oxygen concentrations led to slower reactions. The coal consumption rate within each segment was determined based on the local oxygen concentration and the relative coal content, as described in Eq.8. When both the coal content and oxygen concentration are sufficient, the coal consumption rate is controlled by chemistry, however, when either the coal content or oxygen concentration is insufficient, the coal consumption rate is determined by the lesser of the two. These rate descriptions in Eq.8 were necessary to avoid numerical errors at low oxygen and coal concentrations.

$$\dot{m}'_{coal} = \begin{cases} -\dot{\omega}' \cdot m_{coal} \\ -\dfrac{\varepsilon \rho_g \pi r^2 C_{O_2}}{v_{O_2} \Delta t}, & \dot{\omega}' m_{coal} \Delta t < m_{coal} \\ -\dfrac{m_{coal}}{\Delta t}, & \dot{C}_{O_2} \Delta t < C_{O_2} \end{cases} \quad (8)$$

Because the oxygen diffusivity and stoichiometry were unknown, it was necessary to obtain the optimal values for the oxygen diffusion factor (k) and stoichiometric

coefficient (v_{O2}) in all calculations accounting for diffusion. A forward solution method was used. First, these two parameters were bounded by reasonable ranges. The oxygen diffusion coefficient (D) was bounded between 10^{-4} to 10^{-6} m²/s, which resulted in a k search range between -10.5 to -9. The search range for v_{O2} was between 0 to 3. Then, both parameters were evaluated one by one with a step size of 0.1 within the corresponding search ranges to calculate the mass loss and fitting error against experimental results (Eq.5). Finally, the optimal parameters were identified by minimizing the fitting errors. Note that the optimal kinetic parameters identified in Section 3.1 (i.e., m, n, A, and E in Eq.2) were used in all reactive transport calculations.

2.3 Note on temporal discretization, Δt

While the TGA data was collected every 0.5 s, the calculation time step was defined as $\Delta t = 0.5/p$. The value of p was chosen to guard against numerical errors (i.e., by satisfying Eq.9), where p was related to the inlet oxygen concentrations and the number of spatial segments (w). To ensure the equations were rigorously discretized in time, the value of p was multiplied by 1.5, as shown in Eq.10. Since the range of oxygen diffusion coefficients chosen was between 10^{-4} and 10^{-6} m²/s, D_{max} in Eq.10 was set to 10^{-4} m²/s to achieve a sufficiently fine time discretization.

$$D\frac{\Delta C_{O_2}}{(h/w)^2}\cdot 0.5 < p \qquad (9)$$

$$p = 1.5\cdot D_{max}\frac{\Delta C_{O_2}}{(h/w)^2}\cdot 0.5 \qquad (10)$$

3. Results and discussion

3.1 TGA results

Fig.3 shows the measured TG and DTG curves from coal samples under different inlet oxygen concentrations. As shown in Fig.3, with decreasing oxygen concentration, the peak reactions gradually shifted towards higher temperatures with slower reaction rates. Fig.3 shows that the key trends in these TG curves can be delineated into three stages. Stages I and II correspond to moisture evaporation and oxygen adsorption, respectively, which both exhibited slow reaction rates. Variations

in these stages were minimal and primarily attributed to sample variability, and only slightly influenced by oxygen diffusion. Stage III represents high temperature coal combustion, where the reaction rate sharply increased, and the influence of oxygen diffusion was most significant. This study therefore focused on the impact of oxygen diffusion effects in Stage III.

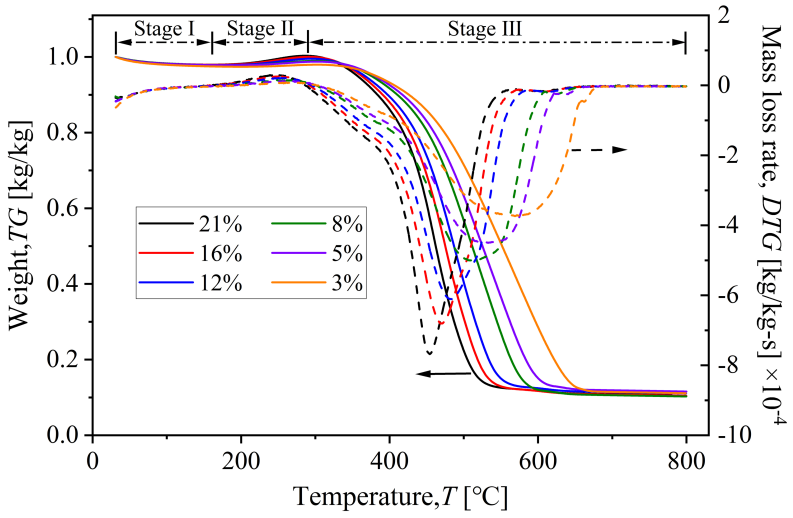

Fig.3 TG and DTG curves obtained with varying inlet oxygen concentrations. Solid and dashed lines represent TG and DTG results, respectively.

In most TGA studies without considering oxygen diffusion, the kinetic parameters obtained at ambient oxygen concentration (i.e., 21%) are used to define the combustion kinetic parameters [17, 25-28]. This classic approach was used also in this study. That is, the effect of oxygen diffusion was assumed to be negligible at ambient oxygen inlet concentration. A GA reverse solving method based on Eqs.1-5 was used to obtain the optimal kinetic parameters (i.e., m, n, A, and E in Eq.2). As shown in Fig.4a, the experimental and calculated TG and DTG curves at these conditions were well-aligned. The TG and DTG curves at lower inlet oxygen concentrations were then calculated using these ambient kinetic parameters without oxygen diffusion effects.

Fig.4b shows that the calculated reaction rates at lower oxygen inlet concentrations were higher than measured, and the fittings worsened as oxygen concentrations decreased. This poor fitting could be due to two reasons: 1) the obtained kinetic parameters were overestimated compared to the actual reaction mechanisms at low

oxygen concentrations; 2) the actual oxygen concentrations throughout the coal samples were lower than the inlet oxygen concentrations due to oxygen diffusion effects. While 1) would require a more rigorous approach in estimating the kinetic parameters, e.g., as in [25-27], 2) would require coupled reactive transport calculations (i.e., as shown in Section 3.2).

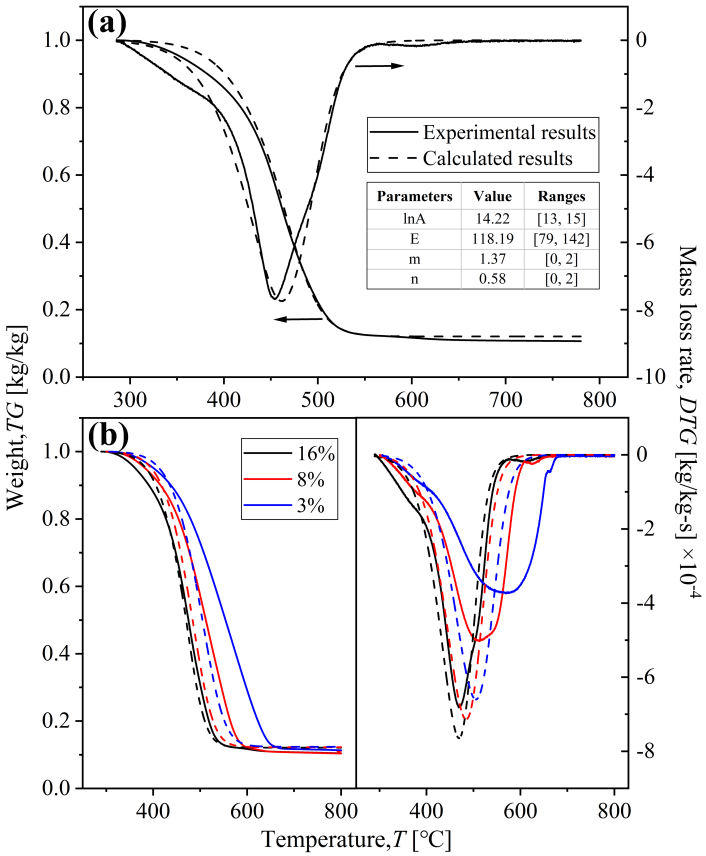

Fig.4 TG-DTG curves measured and calculated using optimal kinetic parameters from coal combustion at ambient conditions at various oxygen concentrations: (a) 21% and (b) 3%, 8%, and 16%. The table in (a) notes optimized kinetic parameters and GA search ranges, and the solid and dashed lines represent measured and calculated results, respectively. Only three oxygen concentrations are shown in (b) for clarity; where the results for 12% and 5% followed the trends shown.

3.2 Optimizing diffusion parameters

To evaluate the optimum number of segments (w), this study evaluated the sensitivities to w = 2, 3, 5, 10, 15, and 20. Fig.5a shows the calculation errors (Eq.5) at different k and v_{O2} combinations with 16% inlet oxygen concentration and w = 10. The results under other oxygen concentrations were similar. From Fig.5a, multiple optimal v_{O2} and k combinations can be identified that minimize calculation errors. Moreover, the minimum calculation errors under different optimal v_{O2} and k combinations are nearly equal. Fig.5b shows multiple optimal combinations at 16% oxygen concentration and different w. This graph shows that the relationship between the optimal combinations is relatively insensitive to spatial discretization when $w \geq$ 10. Therefore, the value of w in this study was set to 10. Fig.5c shows optimal combinations under different oxygen concentrations with w = 10. This figure shows that there is an exponential relationship between k and v_{O2}.

Figs.5b and 5c underscore a key relationship, i.e., the optimal v_{O2} increases with k. Physically, this implies that the oxygen consumption increases with the oxygen diffusion rate. This relationship reflects the fact that GA optimization methods do not reveal unique solutions. However, these figures do show excellent fitting results across a reasonable range of stoichiometry and diffusivity values. This is a key result that suggests how oxygen diffusion may indeed influence TGA results.

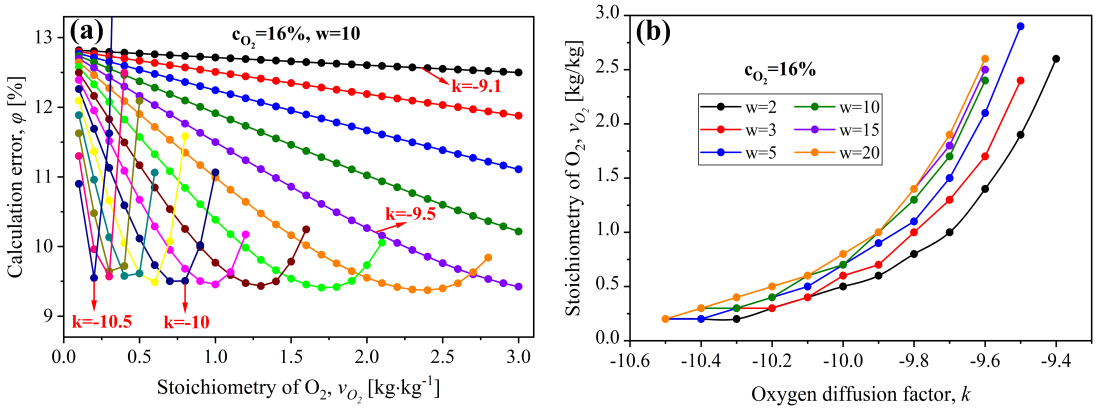

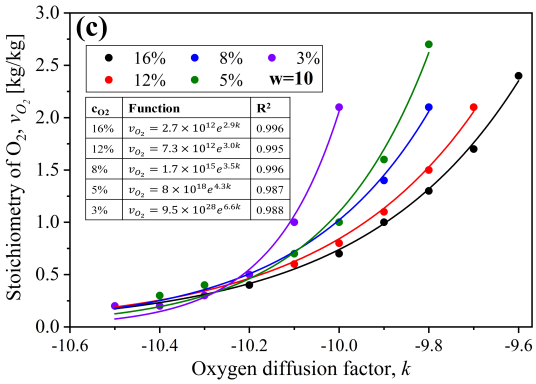

Fig.5 Calculated results under different parameters. (a) Calculation errors under different k and v_{O2} for 16% oxygen concentration with w=10; (b) optimal k and v_{O2} combinations at 16% oxygen concentration for different values of w; (c) optimal k and v_{O2} combinations under various oxygen concentrations with w=10.

3.3 Oxygen concentration distributions

Fig.6 shows the calculated TG and DTG curves with oxygen diffusion effects at minimal calculation errors. This figure shows great improvements in the fittings compared to Fig.4b, where only chemistry was considered. However, there were still slight deviations, especially near the maximum reaction rates, and the fitting error increased with decreasing oxygen concentrations. This poor fitting may be due to the model simplifications. For example, a one-step equation was used to describe the complex coal combustion process, assuming a constant oxygen stoichiometric coefficient under varying oxygen concentrations. Moreover, the optimal kinetic parameters were obtained at 21% oxygen concentration without considering oxygen diffusion effects. Nevertheless, the improvements between Fig.4b and Fig.6 do demonstrate how oxygen diffusion effects can influence thermal degradation of combustible porous media in TGA experiments.

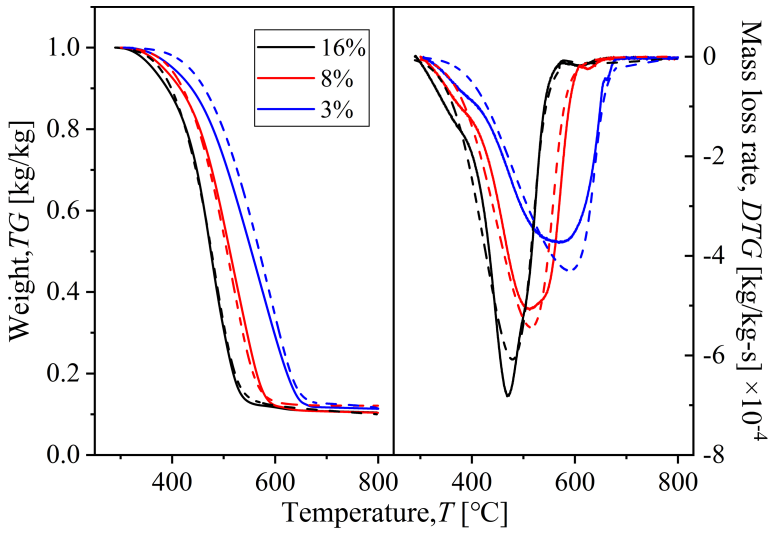

Fig.6 TG-DTG curves measured and calculated with oxygen diffusion effects at various oxygen concentrations. The solid and dashed lines represent measured and calculated results, respectively. Only three oxygen concentrations are shown for clarity; where the results for 12% and 5% followed the trends shown.

Fig.7a shows the calculated oxygen concentration profiles with temperature at multiple locations and different optimal v_{O2} and k combinations at 16% inlet oxygen concentration. This figure shows that, at the same temperature (and time), the oxygen concentrations gradually decreased within the sample. Within one location, the oxygen concentration i) first decreases, as oxygen is consumed via increasingly intense reactions; and ii) then increases, as the reaction intensity diminishes. Importantly, the oxygen profiles at different optimal combinations are very similar. These similar profiles indicate that, although the GA method yields non-unique optimal combinations, the characteristic oxygen profiles do appear reasonably unique. This result provides confidence that this novel method provided physically meaningful results regarding how oxygen diffusion affected TGA results.

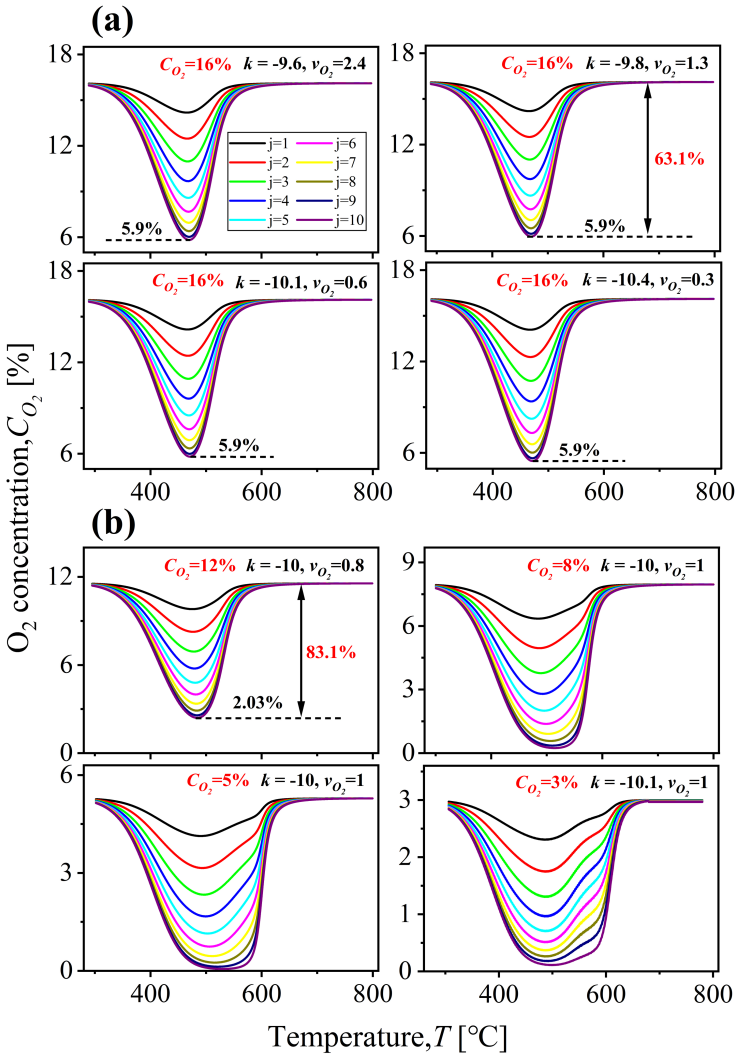

Fig.7 Oxygen concentration profiles under various optimal v_{O2} and k combinations in TGA samples with different oxygen concentrations, i.e., (a) 16% and (b) 12%, 8%, 5%, and 3%.

Fig.7b shows that the results at lower inlet oxygen concentrations followed similar characteristic profiles but dipped to lower concentrations. That is, at 16% and 12% inlet oxygen concentrations, oxygen diffusion effects caused maximum oxygen concentration differences of approximately 63% and 83%, respectively, relative to their inlet concentrations. When inlet oxygen concentrations were below 10%, the minimum oxygen concentrations at the base of the sample were near 0%. At these

minimum oxygen concentrations, plateaus in the oxygen profiles were simulated. These plateaus reflect the time in the TGA experiment when the mass loss rate was limited by oxygen transport, as transport dynamics – unlike the chemistry – are relatively insensitive to temperature [20]. These plateaus grew with lower inlet oxygen concentrations, which corresponded to an increased time when the TGA mass loss was limited by oxygen transport. Altogether, Fig.7 underscores that, even in TGA experiments following best practices with small particle and sample sizes, it is possible that diffusive effects can lead to dynamic reactant gradients. The resulting mass transport should be accounted for in analyzing the data to better understand how local mass transport affects the thermal degradation of combustible porous media.

4. Conclusion

In this paper, a novel modeling method was developed to quantitatively explore oxygen diffusion effects during the thermal degradation of combustible porous media. By coupling genetic algorithm (GA) optimization with a one-dimensional reactive transport model, this method provided valuable estimations of unknown diffusion and kinetic terms. Using coal as the model fuel, kinetic parameters were first determined from TGA experiments at 21% oxygen concentration without considering oxygen diffusion. Then, with these kinetic parameters fixed, optimal combinations of the oxygen diffusion exponent (k) and stoichiometric number (v_{O2}) were evaluated at lower inlet oxygen concentrations (3-16%) to assess oxygen diffusion effects. Finally, these optimized parameters were used to simulate in-depth oxygen profiles throughout the coal samples at different inlet oxygen concentrations. The following conclusions were drawn:

(1) Although the GA method yields multiple optimal combinations values for k and v_{O2} at each inlet oxygen concentration, which exhibit exponential relationships to each other, the local characteristic oxygen profiles were reasonably unique. This finding suggests that the novel model provided physically meaningful insights into how oxygen diffusion effects impacted thermal degradation of combustible porous media.

(2) With oxygen diffusion, there were significant variations in oxygen concentrations throughout the coal sample, exceeding 63% of the inlet oxygen concentration. When the reference oxygen concentrations were below 10%, oxygen concentrations near 0% were simulated away from the sample surface. These low oxygen concentrations resulted in plateaus in mass loss rates, which implied that the mass loss was limited by oxygen diffusion.

Altogether, this study provides a novel methodology and comprehensive quantitative analysis exploring the potential for oxygen diffusive effects to affect the thermal degradation rates in porous combustible materials. Based on the findings, it appears that oxygen diffusive effects may indeed influence thermal degradation processes, and these effects amplify with decreasing inlet oxygen concentrations. This work is significant for smouldering combustion and thermal degradation processes, including many fire safety problems and emerging applications for waste-to-energy, biochar production, and contaminated soil remediation.

Declaration of competing interest

The authors declare that they have no known competing financial interests or personal relationships that could have appeared to influence the work reported in this paper.

Acknowledgements

This work was principally supported by the National Natural Science Foundation of China (Grant No. 52130411, 52074286). Fei Hou was supported by the China Scholarship Council (Grant No. 202206420074). Additional funding was provided by the Royal Society (RG\R2\232528) and from The Open University through Engineering & Innovation Research Funding, Higher Education Innovation Funding Knowledge Transfer Vouchers, and the Open Societal Challenges Programme in support of the SPLICE challenge.

References

[1] J.L. Torero, J.I. Gerhard, M.F. Martins, M.A.B. Zanoni, T.L. Rashwan, J.K. Brown, Processes defining smouldering combustion: integrated review and

364 synthesis, *Prog. Energy Combust. Sci.* 81 (2020) 100869.
365 https://doi.org/10.1016/j.pecs.2020.100869.
366 [2] M.A.B. Zanoni, J. Wang, J.L. Torero, J.I. Gerhard, Multiphase modelling of water
367 evaporation and condensation in an air-heated porous medium, *Appl. Therm. Eng.*
368 212 (2022) 118516. https://doi.org/10.1016/j.applthermaleng.2022.118516.
369 [3] Y. Tang, X. Zhong, G. Li, Z. Yang, G. Shi, Simulation of dynamic temperature
370 evolution in an underground coal fire area based on an optimised thermal-hydraulic-
371 chemical model, *Combust. Theory Model.* 23(1) (2019) 127-146.
372 https://doi.org/10.1080/13647830.2018.1492742.
373 [4] T.L. Rashwan, T. Fournie, M. Green, A.L. Duchesne, J.K. Brown, G.P. Grant, J.L.
374 Torero, J.I. Gerhard. Applied smouldering for co-waste management: Benefits and
375 trade-offs. *Fuel Process. Technol.* 240 (2023) 107542.
376 https://doi.org/10.1016/j.fuproc.2022.107542.
377 [5] T.L. Rashwan, M.A.B. Zanoni, J.H. Wang, J.L. Torero, J.I. Gerhard. Elucidating
378 the characteristic energy balance evolution in applied smouldering systems. *Energy*
379 273 (2023) 127245. https://doi.org/10.1016/j.energy.2023.127245.
380 [6] T.L. Rashwan, T. Fournie, J.L. Torero, G.P. Grant, J.I. Gerhard. Scaling up self-
381 sustained smouldering of sewage sludge for waste-to-energy. *Waste Manage.* 135
382 (2021) 298-308. https://doi.org/10.1016/j.wasman.2021.09.004.
383 [7] A. Boateng, M. Garcia-Perez, O. Mašek, R.C. Brown, B.D. Campo, Biochar
384 production technology. *Edited by Routledge*. (2015) 85-110.
385 [8] D. Berslin, A. Reshmi, B. Sivaprakash, N. Rajamohan, P.S. Kumar, Remediation
386 of emerging metal pollutants using environment friendly biochar- Review on
387 applications and mechanism. *Chemosphere*. 290 (2022) 133384.
388 https://doi.org/10.1016/j.chemosphere.2021.133384.
389 [9] Z.W. Gan, L. J. Deng, J.Y. Wang, G.Y. Cheng, C. Zhao, Z.P. Zhang, Y.Z. Li, Z.L.
390 Song. Method of smoldering combustion for the treatment of oil sludge-
391 contaminated soil. *Waste Manage.* 175 (2023) 73-82.
392 https://doi.org/10.1016/j.wasman.2023.12.048.

[10] R. Solinger, G. P. Grant, G. C. Scholes, C. Murray and J. I. Gerhard. 2020. STARx Hottpad for smoldering treatment of waste oil sludge: Proof of concept and sensitivity to key design parameters. *Waste Manage Res.* 38 (2020). 554-566. https://doi.org/10.1177/0734242X20904430.

[11] G.C. Scholes, J.I. Gerhard, G.P. Grant, D.W. Major, J.E. Vidumsky, C. Switzer, J.L. Torero. Smoldering Remediation of Coal-Tar-Contaminated Soil: Pilot Field Tests of STAR. *Environ Sci Technol.* 49 (2015) 14334-14342. https://doi.org/10.1021/acs.est.5b03177.

[12] P. Pironi, C. Switzer, J.I. Gerhard, G. Rein, J.L. Torero. Self-Sustaining Smoldering Combustion for NAPL Remediation: Laboratory Evaluation of Process Sensitivity to Key Parameters. *Environ Sci Technol.* 45 (2011) 2980-2986. https://doi.org/10.1021/es102969z.

[13] K.K. Dwivedi, Prabhansu, M.K. Karmakar, P.K. Chatterjee, Thermal degradation, characterization and kinetic modeling of different particle size coal through TGA, *Therm. Sci. Eng. Prog.* 18 (2020) 100523. https://doi.org/10.1016/j.tsep.2020.100523.

[14] A. Mlonka-Mędrala, A. Magdziarz, T. Dziok, M. Sieradzka, W. Nowak, Laboratory studies on the influence of biomass particle size on pyrolysis and combustion using TG GC/MS, *Fuel* 252 (2019) 635-645. https://doi.org/10.1016/j.fuel.2019.04.091.

[15] L. Ma, L. Zhang, D. Wang, H. Xin, Q. Ma, Pore structure evolution during lean-oxygen combustion of pyrolyzed residual from low-rank coal and its effect on internal oxygen diffusion mechanism, *Fuel* 319 (2022) 123850. https://10.1016/j.fuel.20 22.123850.

[16] F. Hou, X. Zhong, M.A.B. Zanoni, T.L. Rashwan, J.L. Torero. Multi-step scheme and thermal effects of coal smouldering under various oxygen-limited conditions. *Energy.* (2024) 131421. https://doi.org/10.1016/j.energy.2024.131421.

[17] H. Yuan, F. Richter, G. Rein, A multi-step reaction scheme to simulate self-heating ignition of coal: Effects of oxygen adsorption and smouldering combustion, *Proc. Combust. Inst.* 38(3) (2021) 4717-4725. https://10.1016/j.proci.2020.07.016.

[18] X. Huang, G. Rein, Smouldering combustion of peat in wildfires: Inverse modelling of the drying and the thermal and oxidative decomposition kinetics, *Combust. Flame* 161(6) (2014) 1633-1644. https://10.1016/j.combustflame.2013.12.013.

[19] W. Lu, B. Guo, G. Qi, W. Yang, Thermal Decomposition Model and Its Reaction Kinetic Parameters for Coal Smoldering with the Use of TG Tests in Oxygen-depleted Air, *Combust. Sci. Technol.* (2021). https://10.1080/00102202.2019.1684910.

[20] S.M. Dakka, G.S. Jackson, J.L. Torero, Mechanisms controlling the degradation of poly (methyl methacrylate) prior to piloted ignition, *Proc. Combust. Inst.* 29(1) (2002) 281-287. https://doi.org/10.1016/S1540-7489(02)80038-4.

[21] Z. Song, X. Huang, M. Luo, J. Gong, X. Pan, Experimental study on the diffusion–kinetics interaction in heterogeneous reaction of coal, *J. Therm. Anal. Calorim.* 129(3) (2017) 1625-1637. https://doi.org/10.1007/s10973-017-6386-1.

[22] Y. Zhang, Y. Zhang, Y. Li, X. Shi, Y. Zhang, Heat effects and kinetics of coal spontaneous combustion at various oxygen contents, *Energy* 234 (2021) 121299. https://10.1016/j.energy.2021.121299.

[23] X. Zhong, L. Li, Y. Chen, G. Dou, H. Xin, Changes in Thermal Kinetics Characteristics during Low-Temperature Oxidation of Low-Rank Coals under Lean-Oxygen Conditions, *Energy Fuels* 31(1) (2017) 239-248. https://doi.org/10.1021/acs.energyfuels.6b02197.

[24] J. Deng, Q. Li, Y. Xiao, H. Wen, The effect of oxygen concentration on the non-isothermal combustion of coal, *Thermochim. Acta* 653 (2017) 106-115. https://doi.org/10.1016/j.tca.2017.05.020.

[25] Z. Song, Modelling oxygen-limited and self-sustained smoldering propagation: Underground coal fires driven by thermal buoyancy, *Combust. Flame* 245 (2022) 112382. https://doi.org/10.1016/j.combustflame.2022.112382.

[26] M.A.B. Zanoni, G. Rein, L. Yermán, J.I. Gerhard, Thermal and oxidative decomposition of bitumen at the Microscale: Kinetic inverse modelling, *Fuel* 264 (2020) 116704. https://doi.org/10.1016/j.fuel.2019.116704.

[27] H. Yuan, F. Restuccia, G. Rein, Computational study on self-heating ignition and smouldering spread of coal layers in flat and wedge hot plate configurations, *Combust. Flame* 214 (2020) 346-357. https://doi.org/10.1016/j.combustflame.2019.12.041.

[28] S. Wessling, W. Kessels, M. Schmidt, U. Krause, Investigating dynamic underground coal fires by means of numerical simulation, *Geophys. J. Int.* 172(1) (2008) 439-454. https://doi.org/10.1111/j.1365-246X.2007.03568.x.